

Caenorhabditis elegans BAF-1 and its kinase VRK-1 participate directly in post-mitotic nuclear envelope assembly

Mátyás Gorjánác^{1,5}, Elke PF Klerkx^{2,5},
Vincent Galy^{1,4}, Rachel Santarella¹,
Carmen López-Iglesias³, Peter Askjaer^{1,2,*}
and Iain W Mattaj^{1,*}

¹European Molecular Biology Laboratory, Heidelberg, Germany,

²Institute for Research in Biomedicine, Barcelona Science Park IRB-PCB, Barcelona, Spain and ³University of Barcelona, Barcelona Science Park SCT-UB, Barcelona, Spain

Barrier-to-autointegration factor (BAF) is an essential, highly conserved, metazoan protein. BAF interacts with LEM (LAP2, emerin, MAN1) domain-carrying proteins of the inner nuclear membrane. We analyzed the *in vivo* function of BAF in *Caenorhabditis elegans* embryos using both RNA interference and a temperature-sensitive *baf-1* gene mutation and found that BAF is directly involved in nuclear envelope (NE) formation. NE defects were observed independent of and before the chromatin organization phenotype previously reported in BAF-depleted worms and flies. We identified vaccinia-related kinase (VRK) as a regulator of BAF phosphorylation and localization. VRK localizes both to the NE and chromatin in a cell-cycle-dependent manner. Depletion of VRK results in several mitotic defects, including impaired NE formation and BAF delocalization. We propose that phosphorylation of BAF by VRK plays an essential regulatory role in the association of BAF with chromatin and nuclear membrane proteins during NE formation.

The EMBO Journal (2007) 26, 132–143. doi:10.1038/sj.emboj.7601470; Published online 14 December 2006

Subject Categories: signal transduction; cell cycle

Keywords: chromosome segregation; LEM proteins; mitosis; nuclear envelope; nuclear pore complex

Introduction

The nuclear envelope (NE) of eukaryotic cells separates the nucleoplasm from the cytoplasm and serves additional essential functions, such as anchoring of chromatin within the nucleus, nuclear stability and positioning of the nucleus

*Corresponding authors. P Askjaer, Cell Division Group, Institute for Research in Biomedicine, Parc Científic de Barcelona, C/Josep Samitier 1-5, Barcelona 08028, Spain. Tel.: +34 93 403 70 18; Fax: +34 93 403 71 09; E-mail: paskjaer@pcb.ub.es or IW Mattaj, European Molecular Biology Laboratory, Meyerhofstrasse 1, 69117 Heidelberg, Germany; E-mail: mattaj@embl.de

⁴Present address: Institut Pasteur, 25 rue du Docteur Roux 75724, Paris cedex 15, France

⁵These authors contributed equally to this work

Received: 25 July 2006; accepted: 6 November 2006; published online: 14 December 2006

(Hetzer *et al.*, 2005). The interphase NE is composed of an outer membrane (ONM) and an inner nuclear membrane (INM), which are joined at nuclear pore complexes (NPCs) that consist of multiple copies of approximately 30 different nucleoporins (Hetzer *et al.*, 2005; Prunuske and Ullman, 2006). The NE is joined via integral INM and ONM proteins to the nuclear lamina, chromatin and the cytoskeleton (Gruenbaum *et al.*, 2005). In metazoa, this entire set of peripheral NE structures is dispersed during mitosis and reassembled during anaphase and telophase. Specifically, INM proteins dissociate from chromatin and the lamina and are dispersed throughout the mitotic endoplasmic reticulum (ER) network from NE breakdown to NE reassembly (Hetzer *et al.*, 2005; Prunuske and Ullman, 2006). MAN1 and emerin are INM proteins belonging to the LEM domain family (Lin *et al.*, 2000) and have been proposed to undergo essential interactions with each other and with lamin and chromatin-associated proteins early during NE assembly (Gruenbaum *et al.*, 2002; Liu *et al.*, 2003; Mansharamani and Wilson, 2005; Margalit *et al.*, 2005). Some LEM domain proteins are conserved in animals, but the family is absent from unicellular eukaryotes and plants. Imaging studies of live cells expressing fluorescently labeled INM proteins have shown that they are mobile during mitosis, but that their mobility is dramatically reduced when they reach the INM, presumably owing to their interaction with the immobile lamina or chromatin-associated proteins (reviewed in Hetzer *et al.*, 2005). Barrier-to-autointegration factor (BAF) is an essential 10 kDa protein that is highly conserved among metazoa (Segura-Totten and Wilson, 2004), and biochemical experiments have shown that BAF binds to the LEM domain of LAP2, emerin and MAN1, suggesting that all LEM domain-carrying proteins may bind BAF (Lee *et al.*, 2001; Shumaker *et al.*, 2001; Furukawa *et al.*, 2003; Mansharamani and Wilson, 2005).

Adding excess BAF to an *in vitro* nuclear assembly reaction hypercondenses chromatin and inhibits NE formation (Segura-Totten *et al.*, 2002). Paradoxically, RNA interference (RNAi)-mediated or genetic inactivation of BAF from *Caenorhabditis elegans* or *Drosophila melanogaster* also causes chromatin hypercondensation that results in segregation defects, including the production of anaphase chromatid bridges that were suggested to lead secondarily to the NE defects observed (Zheng *et al.*, 2000; Furukawa *et al.*, 2003). As an anaphase bridge phenotype can be caused by altering many different processes, including the spindle assembly checkpoint (Lew and Burke, 2003) and DNA replication (Meier and Ahmed, 2001), the absence of BAF might affect processes distinct from chromatin organization. Co-depletion of both emerin and the MAN1-related protein LEM-2 from *C. elegans* with RNAi produces a similar phenotype (Liu *et al.*, 2003). The anaphase chromatid bridges retain mitotic histone H3 phosphorylation and do not appear to associate with reassembling nuclear membranes. Furthermore, removal of

either lamin or BAF alone or co-depletion of emerin and LEM-2 affects the interphase distribution of the other proteins in this group (Liu *et al*, 2000; Gruenbaum *et al*, 2002; Liu *et al*, 2003; Margalit *et al*, 2005). This led to the proposal that these proteins are mutually required for the integrity of the NE during interphase (Margalit *et al*, 2005).

During mitosis, several NE components are phosphorylated (Gerace and Blobel, 1980; Macaulay *et al*, 1995), which presumably is a prerequisite for NE breakdown (Heald and McKeon, 1990). While the protein kinase Cdk1/cdc2 has been shown to phosphorylate both lamins and nucleoporins (Peter *et al*, 1990; Macaulay *et al*, 1995), it is conceivable that additional kinases act on NE proteins during mitosis. Indeed, while this work was in progress, it was reported that the human vaccinia-related kinases (VRKs) can phosphorylate BAF in its dimeric form and thereby reduce the interactions between BAF dimers, chromatin and LEM domain proteins (Nichols *et al*, 2006). Moreover, BAF phosphorylation influences interaction between lamin and emerin *in vitro* (Bengtsson and Wilson, 2006).

The fact that over- or underexpression of BAF affects several mitotic processes has hampered precise *in vivo* analysis of its roles. Here we overcome this difficulty by employing a temperature-sensitive *C. elegans* *baf-1* allele in combination with a novel, fast-acting temperature controller and time-lapse microscopy. Increasing temperature

after anaphase onset allowed discrimination of BAF's roles in NE assembly and chromatin segregation. BAF is shown to act directly on NPC and NE formation. Additionally, we identify VRK as an essential regulator of BAF and NE assembly.

Results

Identification of a point mutation in the *C. elegans* *baf-1* gene

To investigate post-mitotic NE formation, we analyzed genetic mutations that cause pronuclear and nuclear appearance (*pna*) defects when visualized by differential interference contrast (DIC) microscopy (Gönczy *et al*, 1999). We mapped the *pna-1(t1639)* mutation to the *baf-1* gene, which encodes the *C. elegans* homologue of BAF. We refer to *pna-1* as *baf-1*. Sequencing *baf-1(t1639)* mutant uncovered a single base-pair substitution that changed the *baf-1* coding sequence and resulted in the substitution of Gly at position 38 by Asp (G38D). G38 is highly conserved across metazoan species and may therefore be important for BAF function. When grown at 20°C or higher, homozygous *baf-1(t1639)* animals produced by heterozygous parents developed into adults that produced only nonviable embryos (Gönczy *et al*, 1999; Figure 1B). We refer to these embryos as *baf-1(t1639)* embryos.

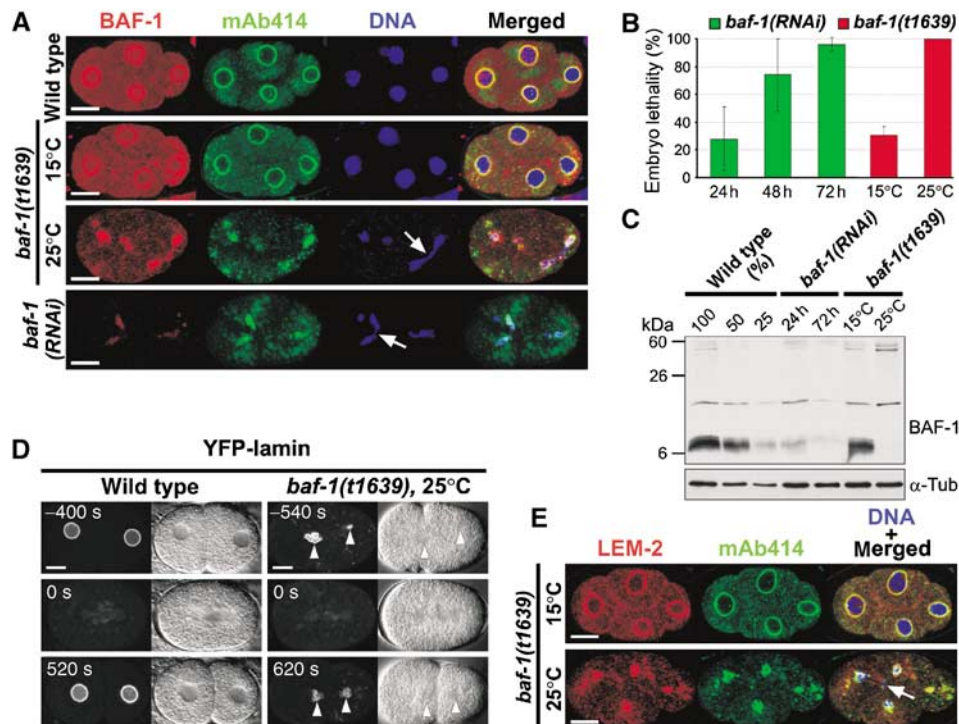


Figure 1 BAF-1 is required for normal nuclear appearance in *C. elegans* embryos. (A) Wild-type, *baf-1(t1639)* (upper, embryo grown at 15°C; lower, embryo at 25°C) and *baf-1(RNAi)* (72 h RNAi) embryos were stained with BAF-1 antiserum, mAb414 and Hoechst to visualize BAF-1, NPCs and chromatin, respectively. Arrows point to chromatin that has failed to segregate correctly. In this and all subsequent figures, embryos are oriented with anterior to the left. (B) Embryonic lethality was determined after 24, 48 and 72 h of RNAi against *baf-1* (green bars) or for *baf-1(t1639)* animals grown at 15 or 25°C (red bars). Average values from 15 animals are shown. Error bars indicate standard deviation. (C) Western blotting was used to compare the amount of BAF-1 in *baf-1(RNAi)* embryos after 24 h (lane 4) and 72 h (lane 5) and BAF-1 G38D in *baf-1(t1639)* embryos grown at 15°C (lane 6) or 25°C (lane 7) with control embryos (lanes 1–3) using BAF-1 antiserum. α -Tubulin antibodies were used as a loading control. (D) Still images from recordings of wild-type and *baf-1(t1639)* embryos expressing YFP-LMN-1 and grown at 25°C. Time in this and subsequent time-lapse recordings is indicated in seconds relative to anaphase onset. Arrowheads point to nuclei with abnormal YFP-lamin distribution. (E) *baf-1(t1639)* embryos grown at 15 or 25°C were stained with LEM-2 antiserum, mAb414 and Hoechst. Bars, 10 μ m.

To confirm that the *baf-1(t1639)* mutant phenotype is due to BAF-1 inactivation, we compared the phenotype of *baf-1(t1639)* mutants and embryos depleted of BAF-1 by RNAi. In both *baf-1(RNAi)* and *baf-1(t1639)* embryos incubated at 25°C, the shape and the size of the nuclei as well as the distribution of nucleoporins recognized by the monoclonal antibody 414 were strongly affected (Figure 1A, compare upper rows with lower rows). Moreover, chromatin segregation was severely compromised with lagging chromosomes and chromatin bridges (Figure 1A, arrows), consistent with previous observations (Zheng *et al*, 2000; Margalit *et al*, 2005).

At 20°C or above, offspring of *baf-1(t1639)* homozygous mutant worms died between the 80- and 100-cell stages. However, when the mutant was grown at 15°C, only 31 ± 6% of the embryos died (Figure 1B). Immunostaining of *baf-1(t1639)* embryos laid at permissive temperature revealed that in most cases, the localization of BAF-1 G38D protein as well as nuclear shape and NPC distribution were similar to wild-type embryos (Figure 1A, two upper rows). In contrast, at the restrictive temperature, BAF-1 G38D was strongly associated with chromatin and did not show nuclear rim staining (Figure 1A, third row). Together, these results suggest that the *baf-1(t1639)* mutant phenotype is indeed due to BAF-1 inactivation and that BAF-1 depletion affects, directly or indirectly, nuclear structure.

Western blotting demonstrated that BAF-1 was present in different isoforms. Multiple bands were present at the size expected for monomeric BAF-1 (10 kDa), but a prominent ~20 kDa band was also detected, most likely corresponding to a dimeric form of BAF-1 resistant to SDS-PAGE (Figure 1C). RNAi confirmed that these bands correspond to BAF-1 and showed furthermore that *baf-1(RNAi)* embryos contained less than 50 and 25% of BAF-1 after 24 and 72 h, respectively, compared with control embryos (Figure 1C). Additional BAF-1 bands were present above 50 kDa, as also observed in vertebrates (Bengtsson and Wilson, 2006). Interestingly, whereas BAF-1 G38D protein from mutant embryos grown at 15°C appeared identical to wild-type protein, BAF-1 G38D from mutant embryos grown at 25°C was almost exclusively present in the higher molecular weight forms, which appeared to be more abundant than in wild-type embryos (Figure 1C, see below).

BAF-1 is essential for NE formation *in vivo*

The presence of a nuclear lamina was investigated using a *C. elegans* strain expressing YFP-fused lamin (LMN-1). In control embryos, YFP-LMN-1 clearly marked the spherical NE during interphase, whereas in *baf-1(t1639)* and *baf-1(RNAi)* embryos, YFP-LMN-1 localization was highly irregular and multilobed (Figure 1D, arrowheads; data not shown). To analyze INM proteins, we stained *baf-1(t1639)* embryos with antibodies against LEM-2 (Figure 1E) or emerlin (Supplementary Figure 1). Both INM proteins showed a sharp NE rim in *baf-1(t1639)* embryos grown at permissive temperature. At restrictive temperature, LEM-2 and emerlin were still recruited to the surface of chromosomes. However, the signals around chromatin were now disorganized and punctate (Figure 1E; Supplementary Figure 1).

The integrity of the NE is essential for the exclusion of macromolecules roughly above 45 kDa. To examine the extent of the defect in BAF-1-depleted embryos, we injected

160 kDa dextran coupled to a fluorochrome into the gonads of either control or BAF-1 RNAi-depleted worms. Although the dextran was always excluded from the interphase nuclei of control embryos (Figure 2A, left panel), it was never excluded from the nuclear space of *baf-1(RNAi)* embryos (Figure 2A, arrow in the right panel). *baf-1(RNAi)* embryos were further tested by examining nuclear exclusion of soluble GFP- β -tubulin. Whereas pronuclei and nuclei of control embryos efficiently excluded soluble GFP- β -tubulin, depletion of BAF-1 by RNAi prevented nuclear exclusion (Figure 3A, two left panels; Figure 3C). These observations confirmed that BAF-1 is required for NE integrity *in vivo*.

Nuclear membranes were next investigated by transmission electron microscopy (TEM). Nuclei of control embryos

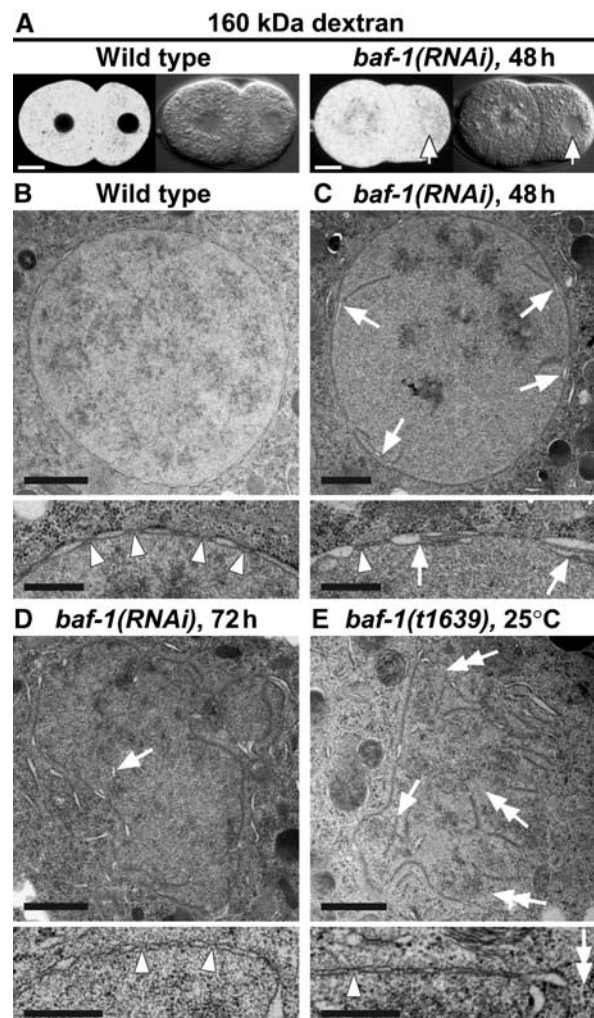


Figure 2 A functional NE is not formed in *baf-1(t1639)* or *baf-1(RNAi)* embryos. (A) 160 kDa fluorescent dextran was injected into gonads of worms and incorporated into oocytes and embryos. While the dextran was excluded from nuclei of a two-cell stage control embryo, 48 h RNAi against BAF-1 prevented formation of functional NEs. Arrows point to a nucleus in the *baf-1(RNAi)* embryo. (B–E) Transmission electron microscopy micrographs of nuclei from wild-type (B), *baf-1(RNAi)* 48 h (C), *baf-1(RNAi)* 72 h (D) and *baf-1(t1639)* at 25°C (E) embryos. Arrowheads point to NPCs. Arrows indicate intranuclear membranes; double arrows show parts of chromatin not covered by nuclear membranes. Bars; 10 μ m (A); 1 μ m (B–E, upper panels); 400 nm (B–E, lower panels).

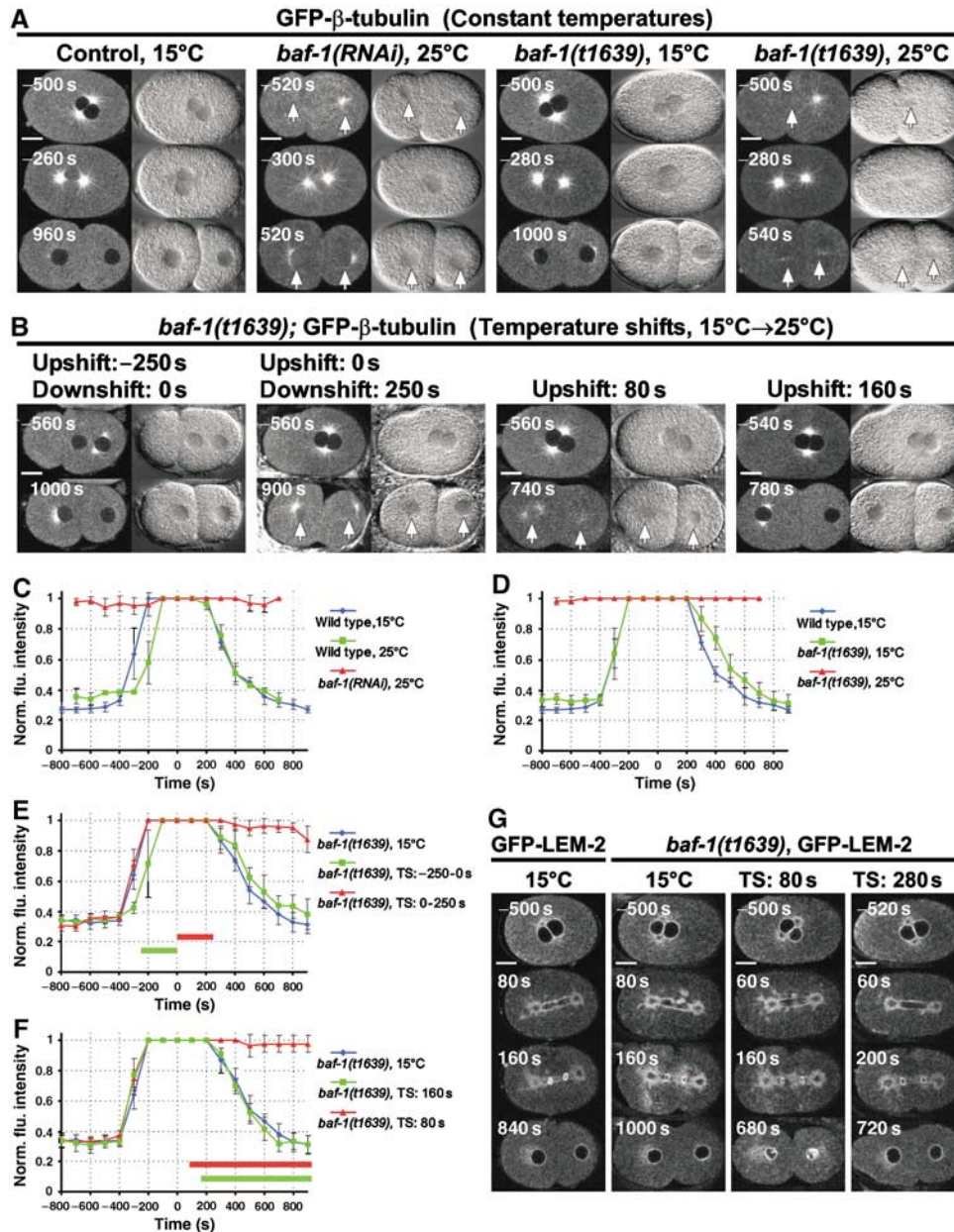


Figure 3 Temperature shifts demonstrate a direct role of BAF-1 in NE assembly. (A) Still images of control, *baf-1(RNAi)* and *baf-1(t1639)* GFP-β-tubulin-expressing embryos grown and recorded at the temperatures indicated. Arrows point to (pro-) nuclei that failed to exclude soluble GFP-β-tubulin. (B) GFP-β-tubulin-expressing *baf-1(t1639)* embryos shifted between 15 and 25°C during recordings at the time points are indicated. Upshift, from 15 to 25°C; downshift, from 25 to 15°C. (C–F) Nuclear exclusion was quantified from time-lapse recordings by dividing nuclear fluorescence intensity by cytoplasmic fluorescence intensity after background subtraction. Time is indicated relative to anaphase onset. TS, temperature shift. For each condition, 3–4 embryos were analyzed. In (E) and (F), red and green bars represent the time period of temperature upshifts corresponding to the appropriate red and green graphs. (G) Localization of GFP-LEM-2 analyzed in wild-type and *baf-1(t1639)* embryos. Embryos were kept stably at 15°C or shifted from 15 to 25°C, either 80 or 280 s after anaphase onset. Bars, 10 μm.

were enclosed by NEs with abundant, regularly spaced NPCs (Figure 2B, arrowheads in magnification). After 48 h of BAF-1 RNAi, invaginations of the inner nuclear membrane into the nuclear space were observed (Figure 2C, arrows), whereas after 72 h, the nuclear shape was dramatically distorted and ribosomes were detected inside the nuclei (Figure 2D). In *baf-1(t1639)* mutants grown at 25°C, the nuclear structure was even more disrupted and irregular, with areas of chromatin not covered by nuclear membranes (Figure 2E, double arrows). Chromatin was still partially associated with membranes and although NE was still clearly definable from rough

ER and NPCs were present, closed NEs were not observed. Thus, both depletion of BAF-1 by RNAi and mutation of BAF-1 at residue G38 prevent enclosure of chromatin and the proper organization of nuclear membranes into a single, continuous NE.

NE formation defects in *baf-1(t1639)* and *baf-1(RNAi)* embryos are direct

Loss of BAF from *C. elegans* embryos or *D. melanogaster* larvae has been reported to cause chromatin condensation and segregation defects (Zheng *et al*, 2000; Furukawa *et al*,

2003; Supplementary Figure 2). It was therefore important to determine whether the NE assembly defects seen in the *baf-1(t1639)* mutant embryos were direct or secondary. Whereas *baf-1(t1639)* embryos at 15°C excluded soluble GFP- β -tubulin from pronuclei and nuclei (Figure 3A, compare first and third panels; Figure 3D), mutant embryos at 25°C failed to do so (Figure 3A, right panel; Figure 3D). By utilizing a novel fast response temperature controller that allows temperature shifts at rates of $\sim 1^\circ\text{C/s}$, we shifted *baf-1(t1639)* embryos rapidly from 15 to 25°C at different cell cycle stages, enabling us to analyze NE assembly at restrictive temperature after allowing normal chromatin segregation to occur at permissive temperature. When *baf-1(t1639)* mutants were shifted from 15 to 25°C at the pronuclear stage, -250 s relative to anaphase onset, and shifted back to 15°C at anaphase onset (0 s), the daughter nuclei excluded soluble GFP- β -tubulin, demonstrating that NE reassembly was not affected (Figure 3B, left panel; Figure 3E). However, when the embryos were shifted to 25°C at anaphase onset and shifted back to 15°C after 250 s, the newly formed nuclei did not exclude GFP- β -tubulin (Figure 3B, second panel; Figure 3E). This suggested that BAF-1 function is required during anaphase for NE formation. Importantly, shifting the temperature from 15 to 25°C at 80 s, that is, after chromosome segregation, still prevented formation of functional NEs (Figure 3B, third panel; Figure 3F). Increasing the temperature at 160 s (Figure 3B, right panel; Figure 3F) or later (data not shown) did not affect the formation of a functional NE. This suggests that BAF-1 is specifically required from anaphase onset until chromosomes are completely enclosed by new NEs in telophase.

To further analyze the NE defects, we performed temperature shift experiments in *baf-1(t1639)* embryos expressing GFP-LEM-2. In wild-type and *baf-1(t1639)* embryos at 15°C, GFP-LEM-2 was recruited to the reforming nuclei after 120–140 s of anaphase onset (Figure 3G, two left columns; Supplementary Figure 3). GFP-BAF-1 was reproducibly recruited 20–40 s earlier (Supplementary Figure 3). Shifting the temperature from 15 to 25°C 80 s after anaphase onset caused an irregular distribution of GFP-LEM-2 (Figure 3G, third column), presumably reflecting the defects in NE structure described above. Shifting the temperature from 15 to 25°C after closure of the NE did not cause defects in GFP-LEM-2 distribution (Figure 3G, right column), suggesting that BAF-1 function is needed to assemble, but not to maintain, a functional NE. Further evidence that BAF-1 is directly involved in NE formation, independently of its role in chromatin organization and segregation, was provided by the observations that (1) after shorter RNAi treatment when the amount of BAF-1 protein was less reduced, embryos had no visible segregation defects, but their nuclei did not exclude GFP- β -tubulin (data not shown) and (2) in *baf-1(RNAi)* and *baf-1(t1639)* embryos at restrictive temperature, NE defects were already observed in the sperm pronuclei (Figures 1D and 3A; Supplementary Figure 1A). We conclude that the defective NE formation seen in *baf-1(t1639)* and *baf-1(RNAi)* embryos is not a consequence of a defect in chromatin segregation, and that BAF-1 is needed to assemble, but not to maintain, the NE.

BAF-1 is a phosphoprotein

Western blotting analysis showed that BAF-1 is present in several isoforms (Figure 1C). When analyzed by two-dimen-

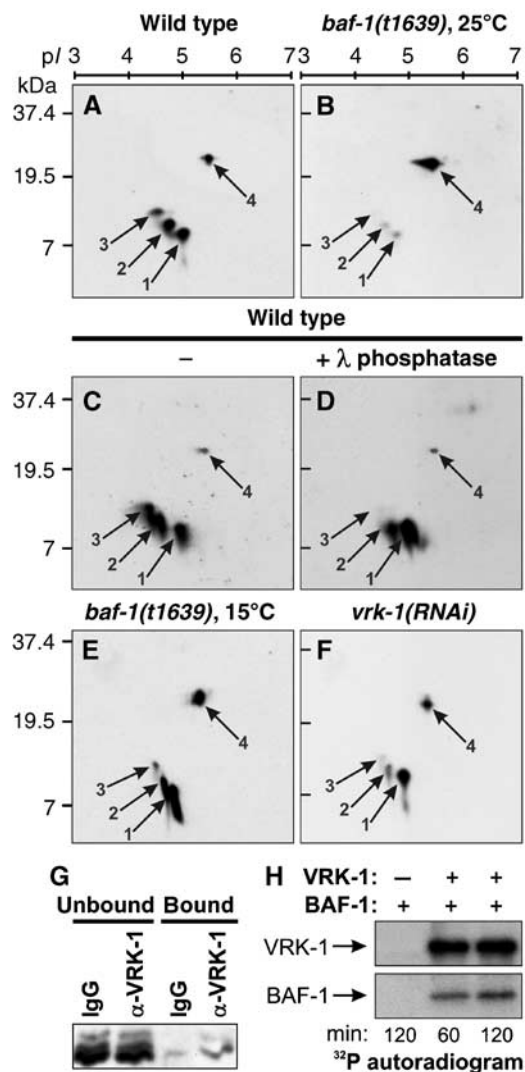


Figure 4 BAF-1 is phosphorylated by VRK-1. (A–F) A 10 μg portion of wild-type embryo extract was untreated (A), mock-treated (C) or λ protein phosphatase-treated (D). Similar extracts from *baf-1(t1639)* mutants grown at 15°C and upshifted to 25°C for 12 h (B) or constantly grown at 15°C (E), or from *vrk-1(RNAi)* embryos (F). The extracts were resolved in two dimensions and immunoblotted with BAF-1 antiserum. Arrows 1–4 indicate different isoforms of BAF-1. Spot 4 is decreased in (C) and (D) owing to slight differences in extract preparation and treatment required for λ protein phosphatase action (see Materials and methods). The linear pI gradient is indicated above the panels, whereas the molecular mass is indicated on the left side of each panel. (G) Wild-type embryo extract was incubated with beads containing either control IgG or VRK-1 antibody. A total of 0.4% of unbound and 33% of bound material was analyzed by immunoblotting with BAF-1 antiserum. (H) *In vitro* phosphorylation reactions containing GST-VRK-1-His and zz-BAF-1-His dimers were performed for 60 or 120 min and analyzed by SDS-PAGE and autoradiography.

sional (2D) gel electrophoresis, wild-type extracts gave rise to four main spots reacting with BAF-1 antiserum (Figure 4A). Three of the spots migrated around 10 kDa (arrows 1–3), whereas a fourth spot migrated at ~ 20 kDa (arrow 4). Treatment of wild-type extracts with λ protein phosphatase led to the disappearance of isoform 3 and a reduction of isoform 2, whereas the relative abundance of isoform 1 increased, demonstrating that BAF-1 is phosphorylated *in vivo* (Figure 4C and D). BAF-1 G38D from *baf-1(t1639)*

embryos grown at 15°C resembled wild-type BAF-1 (Figure 4E), and quantification showed a similar relative abundance of the individual spots 1–4 (BAF-1: 28, 28, 19 and 25%; BAF-1 G38D: 30, 28, 15, and 27%). In contrast, BAF-1 G38D from embryos grown at 15°C and shifted to 25°C for ~12 h was almost entirely present in spot 4 in the 2D gel analysis (Figure 4B; relative abundances of spots 1–4: 17, 14, 3 and 66%) in agreement with our one-dimensional (1D) gel analysis (Figure 1C). λ protein phosphatase treatment did not alter the migration of spot 4, indicating that this isoform of BAF-1 is not phosphorylated (Figure 4C and D). This suggested that the NE phenotypes observed in *baf-1(t1639)* embryos at 25°C may be caused by a lack of phosphorylation of BAF-1, and is consistent with the rapid responses detected in our temperature shift experiments.

BAF-1 is a substrate for the protein kinase VRK-1

The observation that BAF-1 G38D protein is a phosphoprotein raised the question of the identity of the protein kinase acting on BAF-1. Two features made us investigate VRK-1. First, searching WormBase (<http://www.wormbase.org>) for protein kinases potentially regulating nuclear appearance based on DIC phenotypes retrieved *vrk-1* as a candidate (Piano *et al*, 2002). Second, a large-scale yeast two-hybrid study of *D. melanogaster* proteins demonstrated an interaction between the fly homologues of BAF and VRK (Giot *et al*, 2003).

To investigate if VRK-1 is required for phosphorylation of BAF-1 *in vivo*, we prepared extracts from *vrk-1(RNAi)* embryos. One-dimensional gel analysis showed that depletion of VRK-1 did not alter the total amount of BAF-1

(Supplementary Figure 4). However, 2D gel analysis revealed that the relative abundances of phospho-specific isoforms 2 and 3 of BAF-1 were reduced by ~49% in *vrk-1(RNAi)* embryos (Figure 4F; relative abundances of spots 1–4: 42, 18, 6 and 34%). As VRK-1 is likely to have several substrates, the observed hypophosphorylation of BAF-1 could be an indirect effect of VRK-1 depletion. We therefore immunoprecipitated VRK-1 from wild-type embryo extracts to test whether VRK-1 and BAF-1 interact *in vivo*. As seen in Figure 4G, a small fraction of BAF-1 was specifically co-precipitated by anti-VRK-1 antibodies. A final line of evidence that BAF-1 is a substrate for VRK-1 was obtained with purified recombinant proteins, which demonstrated that BAF-1 was phosphorylated by VRK-1 *in vitro* (Figure 4H, lower panel). In addition, VRK-1 was autophosphorylated (Figure 4H, upper panel).

VRK-1 is essential for NE assembly

Combining the observations that BAF-1 is required for NE assembly and that it is a VRK-1 substrate suggested that inhibition of VRK-1 might interfere with NE formation. Initially, the effect of VRK-1 depletion on nuclear lamina formation was examined. Whereas YFP-LMN-1 brightly stained the NE of pronuclei and nuclei of early control embryos (Figure 5A, left), formation of a nuclear lamina did not take place in *vrk-1(RNAi)* embryos (Figure 5A, right). RNAi efficiency was tested with antibodies against VRK-1. In control extracts, the VRK-1 antibodies recognized three bands with apparent molecular masses of ~67, ~80 and ~100 kDa, which were all absent from *vrk-1(RNAi)*

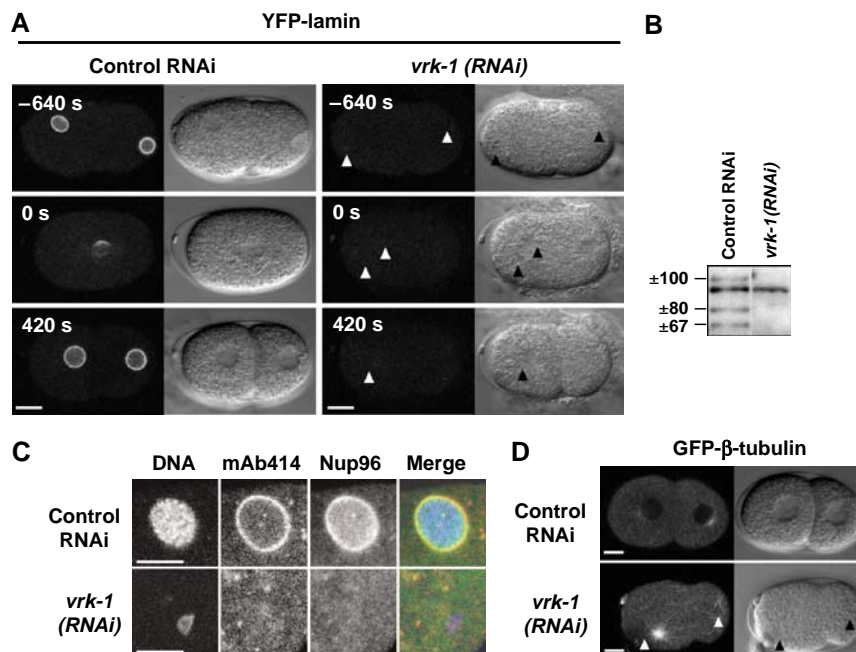


Figure 5 VRK-1 is essential for NE formation. (A) The first mitotic division of control and *vrk-1(RNAi)* embryos expressing YFP-LMN-1 was recorded by time-lapse microscopy. Arrowheads point to (pro-) nuclei in the *vrk-1(RNAi)* embryo. Bars, 10 μ m. (B) Western blot of extracts from control and *vrk-1(RNAi)* embryos with VRK-1 antibodies revealed three isoforms of VRK-1 with estimated molecular weights of ~67, ~80 and ~100 kDa, which were all efficiently depleted by *vrk-1* RNAi. A prominent cross-reacting band of ~90 kDa was detected. (C) Immunofluorescence analysis with mAb414 (red in merge) and Nup96 antibodies (green in merge) showed nuclear rim staining in control but not in *vrk-1(RNAi)* embryos. DNA was visualized with Hoechst (blue in merge). Bars, 5 μ m. (D) Nuclear exclusion assay using GFP- β -tubulin demonstrated that VRK-1 depletion prevented the formation of a functional NE. Images were taken 10 min after the first mitotic anaphase onset. Arrowheads point to nuclei in the *vrk-1(RNAi)* embryo. Bars, 10 μ m.

extracts (Figure 5B). The predicted molecular mass of VRK-1 is 67.3 kDa. The slower migrating bands may correspond to post-translationally modified forms of VRK-1 and/or different splicing isoforms.

Nuclear lamina formation requires nuclear protein import, and we therefore investigated if NPC assembly is dependent on VRK-1 function. To this end, we stained control and *vrk-1(RNAi)* embryos with mAb414 and Nup96 antiserum. Both antibodies gave rise to nuclear rim signal in control embryos, whereas staining was absent from the region surrounding chromatin in *vrk-1(RNAi)* embryos (Figure 5C). Similar results were observed by analysis of GFP-Nup35 and YFP-Nup107 in living embryos by time-lapse microscopy (Supplementary Figure 5). Thus, NPC formation is dependent on VRK-1. Analysis of fixed embryos or of living embryos expressing GFP-histone H2B revealed that chromosome appearance and segregation is abnormal in *vrk-1(RNAi)* embryos (Figure 5C; Supplementary Figure 6). Failure to segregate chromosomes often led to formation of daughter cells with very uneven amounts of DNA, however, this correlated with a high frequency of cleavage furrow regression (13/16 embryos), providing an explanation for the reported cytokinesis defects in *vrk-1(RNAi)* embryos (Piano *et al*, 2002 and data not shown). Finally, comparing embryos 10 min after anaphase onset showed fully grown nuclei excluding GFP- β -tubulin in control embryos, whereas nuclear exclusion was never observed in *vrk-1(RNAi)* embryos (Figure 5D). In conclusion, depletion of VRK-1 prevents formation of a functional NE.

VRK-1 localizes to the NE and controls BAF-1 chromatin association

To understand the relationship between BAF-1 and VRK-1, it was important to determine the dynamics of VRK-1 localization. Previous studies in other species have determined the steady-state localization of VRK proteins and have found VRK mainly in the nucleus, with a small fraction in the cytoplasm and membrane compartments (Nichols and Traktman, 2004; Sevilla *et al*, 2004a,b). We generated three independent strains expressing low levels of VRK-1 fused to the C-terminus of GFP (strain BN5) or GFP-S-peptide (strains BN8 and BN9), all of which showed identical localization (Figure 6A and data not shown). Confocal time-lapse microscopy revealed that GFP-VRK-1 was nuclear during interphase, accumulated at the nuclear rim in prophase and localized to chromatin through meta-, ana- and telophase (Figure 6A, top). Importantly, identical observations were obtained when the localization of endogenous VRK-1 was investigated with VRK-1 antibodies (Figure 6A, bottom). During anaphase, VRK-1 showed increased localization to the so-called 'core' region of chromatin, where spindle microtubules attach (Figure 6A). Interestingly, this localization pattern is reminiscent of BAF in cultured human cells (Haraguchi *et al*, 2001) and BAF-1 in *C. elegans* embryos (below).

The above observations prompted us to examine whether VRK-1 regulates BAF-1 localization. In control embryos, GFP-BAF-1 localized to the NE during interphase, as well as in prophase, before NE breakdown (Figure 6B). Note that GFP-BAF-1 suppresses the defects observed in downregulation of endogenous BAF-1 and is thus functional (Figure 6C). In metaphase, GFP-BAF-1 was absent from chromatin and was recruited ~80 s after anaphase onset to the 'core' region

of chromatin (Figure 6B, see inset). This localization pattern was consistent with our observations using BAF-1 antiserum to detect endogenous BAF-1, as well as with the localization of human BAF (Figure 1A and data not shown; Haraguchi *et al*, 2001). Interestingly, depletion of VRK-1 by RNAi for only 13 h was sufficient to cause strong accumulation of GFP-BAF-1 on chromatin throughout mitosis, indicating that VRK-1 activity is required for BAF-1 to dissociate from mitotic chromatin (Figure 6B). Similarly, analyzing endogenous BAF-1 in *vrk-1(RNAi)* embryos after 13 h showed an increase in chromatin association of BAF-1 in anaphase in the absence of VRK-1 (Figure 6D). To confirm that this abnormal distribution of GFP-BAF-1 is not an indirect consequence of NE defects before mitosis, we depleted GTPase Ran by RNAi. *ran-1(RNAi)* embryos are defective in NE assembly (Askjaer *et al*, 2002); however, GFP-BAF-1 did not accumulate on mitotic chromatin in the absence of Ran (Figure 6B). Expression of mutant GFP-BAF-1 G38D at 25°C induced a phenotype similar to that observed with wild-type BAF-1 in *vrk-1(RNAi)* embryos in that a significant proportion of GFP-BAF-1 G38D remained on chromatin at all mitotic stages (Figure 6B). To examine whether VRK-1 localization was reciprocally dependent on BAF-1, we stained *baf-1(RNAi)* embryos with VRK-1 antiserum. Depletion of BAF-1 did not abolish nuclear localization of VRK-1 (Supplementary Figure 7A). In conclusion, VRK-1 is required for release of BAF-1 from chromatin during mitosis. Mutation of BAF-1 at residue G38 induces a temperature-dependent association with mitotic chromatin, which is similar to the *vrk-1(RNAi)* phenotype.

Depletion of VRK-1 causes constitutive chromatin association of LEM domain proteins

The abnormal presence of BAF-1 on chromatin during mitosis in *vrk-1(RNAi)* embryos might also affect LEM domain protein localization. To test this, VRK-1 was depleted from embryos expressing GFP-LEM-2 or GFP-emerin. This resulted in strong accumulation of GFP-LEM proteins on chromatin at all steps of the cell cycle (Figure 7A, right; Supplementary Figure 7B and data not shown), indicating that VRK-1 is required to dissociate BAF-1 and, thereby, also LEM domain proteins from chromatin during mitosis. The strong recruitment of the transmembrane LEM domain proteins on chromatin in *vrk-1(RNAi)* embryos implied that nuclear membranes were also present on chromatin. Strikingly, TEM analysis revealed that depletion of VRK-1 led to the formation of nuclei largely enclosed by nuclear membranes but almost completely devoid of NPCs (Figure 7B). The TEM analysis also revealed the presence of gaps in the NE that were larger than nuclear pores, and multiple intranuclear vesicular and tubular membrane structures were observed upon depletion of VRK-1 (Figure 7B, arrows). Chromatin appeared more dense and heterochromatin-like. Taken together, our experiments demonstrate that VRK-1 is required for the formation of a functional NE containing NPCs and a lamina. At least some of these effects seem to involve phosphorylation of BAF-1 by VRK-1.

Discussion

The LEM domain INM proteins have been shown to interact specifically with BAF *in vitro* (Furukawa, 1999; Lee *et al*, 2001; Shumaker *et al*, 2001; Mansharamani and Wilson, 2005). Moreover, addition of an excess of either a LEM

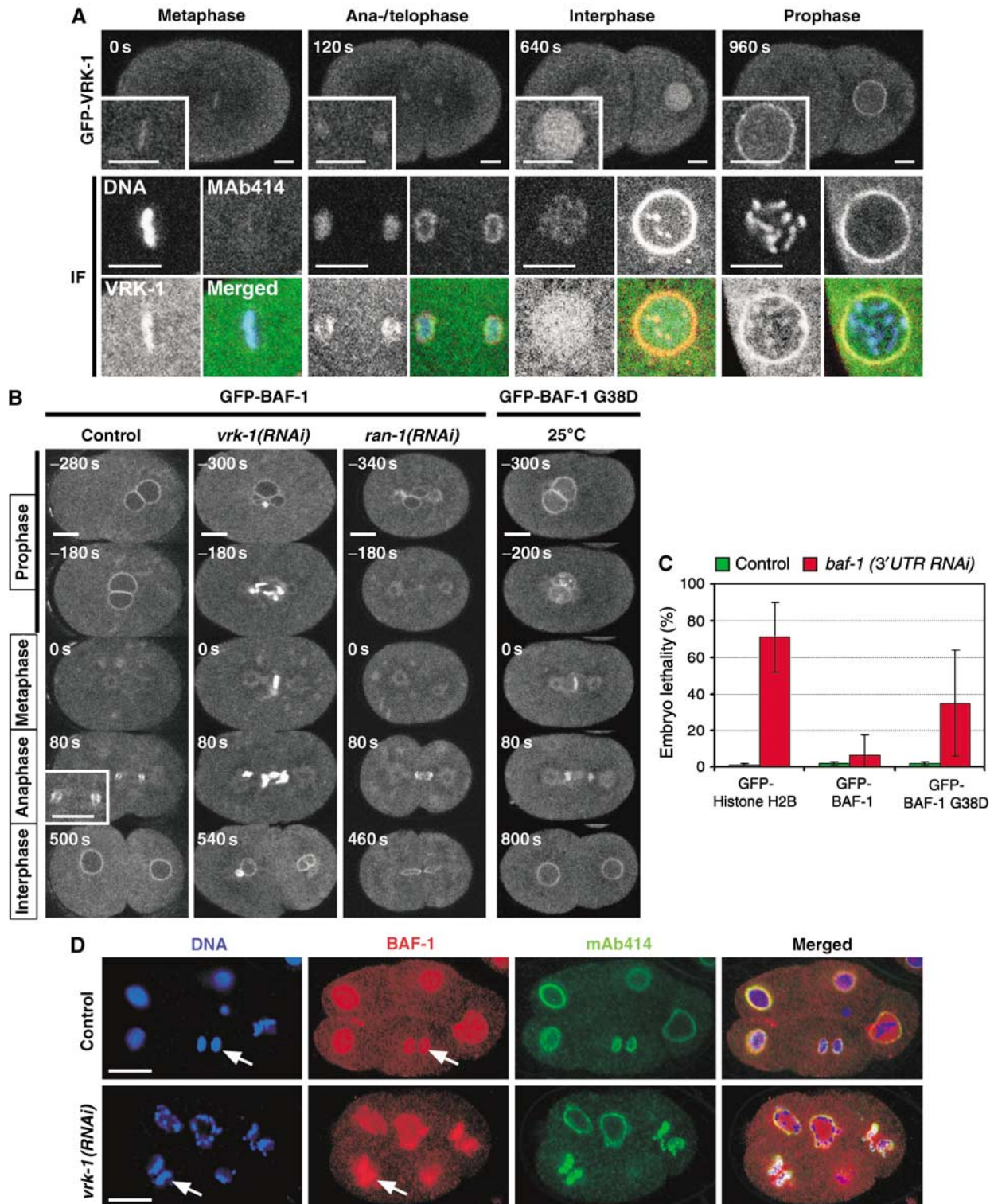


Figure 6 VRK-1 localizes to the NE and controls association of BAF-1 with chromatin. **(A)** Frames from time-lapse recording of an embryo expressing GFP-VRK-1 (top, inset: zoom $\times 3$) and immunofluorescence analysis of fixed embryos (bottom) with mAb414 (red in merge) and VRK-1 (green in merge) together with Hoechst to visualize DNA (blue in merge). Timing in GFP images refer to anaphase onset in live recording; immunofluorescence images where chosen to represent similar time points. Bars, 5 μ m. **(B)** Localization of GFP-BAF-1 and GFP-BAF-1 G38D in control, *vrk-1(RNAi)* and *ran-1(RNAi)* embryos was monitored by time-lapse microscopy (inset shows $\times 2$ magnification of GFP-BAF-1 recruited to the chromatin 'core' region in anaphase). Bar, 10 μ m. **(C)** Embryonic lethality was determined after incubating hermaphrodites expressing GFP-histone H2B, GFP-BAF-1 or GFP-BAF-1 G38D for 72 h with control bacteria (green bars) or bacteria expressing dsRNA corresponding to the 3'UTR of the *baf-1* transcript (red bars). Average values from 15 animals are shown; error bars indicate standard deviation. **(D)** Immunofluorescence analysis with mAb414 and BAF-1 antiserum showed enhanced BAF-1 association with anaphase chromatin (arrows) in *vrk-1(RNAi)* embryos. Bars, 10 μ m.

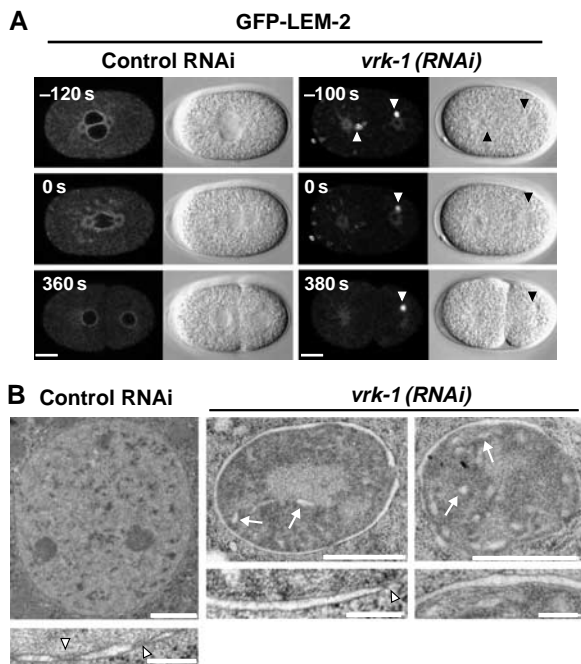


Figure 7 Depletion of VRK-1 abolishes mitotic release of LEM domain proteins and leads to defective assembly of nuclear membranes. **(A)** Time-lapse microscopy of control and *vrk-1(RNAi)* embryos demonstrated that depletion of VRK-1 led to a prominent association of GFP-LEM-2 with (pro-) nuclei (indicated by arrowheads; both nuclei were not always present in the same focal plane) throughout the cell cycle. Bars, 10 μ m. **(B)** Transmission electron microscopy micrographs of nuclei from control and *vrk-1(RNAi)* embryos. In the control embryo, many regularly spaced NPCs were observed in the NE (arrowheads in bottom panels), whereas *vrk-1(RNAi)* embryos contained highly condensed chromatin surrounded by nuclear membranes with no or few NPCs. Arrows point to examples of abundant intranuclear membrane structures in *vrk-1(RNAi)* embryos. Bars, 1 μ m (top panels); 200 nm (bottom panels).

domain-containing fragment (Gant *et al*, 1999) or BAF (Segura-Totten *et al*, 2002) inhibits nuclear assembly and in the case of BAF, chromatin decondensation as well. It had thus been proposed that BAF would be important for NE assembly. However, previous *in vivo* studies in which BAF was depleted from either *C. elegans* embryos (Zheng *et al*, 2000; Margalit *et al*, 2005) or *D. melanogaster* larvae (Furukawa *et al*, 2003) had demonstrated strong effects on chromosome condensation and segregation, including the aberrant retention of mitotic chromatin modification during late anaphase and telophase. Thus, it was essential to determine whether the NE assembly defects observed in *baf-1* embryos were a secondary consequence of defects in chromosome condensation or segregation. We provide three lines of evidence that BAF-1 has a direct effect on NE assembly and function. First, defects were already apparent in sperm pronuclei of *baf-1(t1639)* and *baf-1(RNAi)* embryos, ruling out segregation as a cause of the NE defect. Second, partial depletion of BAF-1 by short RNAi treatment resulted in nuclear defects without visibly affecting chromosome condensation or segregation. Third, switching *baf-1(t1639)* embryos to the non-permissive temperature after chromosome separation consistently and rapidly resulted in NE defects. Therefore, although BAF-1 depletion or mutation affects several processes, the effects on the NE are either upstream to, or independent of, the chromosomal defects.

Phosphorylation of BAF by VRK

Our data show that the protein kinase VRK-1 phosphorylates BAF-1 *in vivo* and thereby regulates BAF-1 localization and function. Depletion of VRK-1 caused NE defects related to those seen in *baf-1(t1639)* and *baf-1(RNAi)* embryos. In general, the phenotypes in *vrk-1(RNAi)* embryos were more severe than in *baf-1(t1639)* and *baf-1(RNAi)* embryos, which we interpret to mean that VRK-1 has additional substrates that are important for NE structure and function. While this work was in progress, Nichols and co-workers showed that human VRKs phosphorylate recombinant human BAF on Ser4, and to a lesser extent on Thr2 and/or Thr3, *in vitro* (Nichols *et al*, 2006). These residues are conserved in *C. elegans* BAF-1.

VRKs were named based on high sequence homology to the vaccinia virus B1 protein kinase, which is essential for viral DNA replication (Rempel and Traktman, 1992). Mammalian genomes encode three VRKs (Nichols and Traktman, 2004), whereas *C. elegans* and *D. melanogaster* each express a single VRK ortholog. Human VRK1 has been shown to phosphorylate p53 (Lopez-Borges and Lazo, 2000), c-Jun (Sevilla *et al*, 2004a) and ATF2 (Sevilla *et al*, 2004b), whereas the *D. melanogaster* VRK ortholog NHK1 phosphorylates the tail of histone H2A (Aihara *et al*, 2004). NHK1 mutants show hypercondensation of chromatin and aberrant spindle formation (Cullen *et al*, 2005; Ivanovska *et al*, 2005). Similarly, *C. elegans vrk-1(RNAi)* embryos display defects in chromatin organization and meiotic and mitotic spindles (Piano *et al*, 2002, our unpublished data). Based on the involvement of BAF in chromatin packing (Zheng *et al*, 2000), we speculate that the chromatin defects induced by VRK-1 depletion in worms or NHK1 mutation in flies may at least in part be caused by hypophosphorylation of BAF.

The residue mutated in *baf-1(t1639)*, Gly38, is conserved in all species (Segura-Totten and Wilson, 2004) and may contribute to BAF dimerization by forming a hydrogen bond with Lys53 in the dimeric partner or by positioning helix 3, which contributes to tight packing of the dimer (Umland *et al*, 2000). Our 2D gel analysis suggests that the Gly38Asp substitution stabilizes BAF-1 dimerization, although further studies are needed to confirm this conclusion.

A role of BAF and VRK in NE assembly

In vitro BAF-1 phosphorylation reduces its binding to chromatin and LEM domain proteins (Bengtsson and Wilson, 2006; Nichols *et al*, 2006). Our observations that mutant BAF-1 protein at the restrictive temperature and wild-type BAF-1 in *vrk-1(RNAi)* embryos, both of which are hypophosphorylated, showed enhanced association with chromatin in mitosis, and that LEM-2 and emerin remain associated with chromatin throughout mitosis in VRK-1-depleted embryos, are consistent with these *in vitro* reports. *In vivo* experiments with overexpression of BAF and VRK proteins in cultured cells have shown that phosphorylation of BAF changes the localization of BAF and emerin, but these studies focused on interphase cells (Nichols *et al*, 2006). Our work thus provides the first *in vivo* evidence for a role of BAF phosphorylation in post-mitotic NE formation. Based on the available data, we propose a model in which phosphorylation of BAF in mitosis is essential to achieve correct timing of recruitment of NE components during NE assembly. At entry into mitosis, BAF

is phosphorylated by VRK and thus dissociates from chromatin. Our observation that VRK accumulates at the nuclear rim immediately before NE breakdown is consistent with this hypothesis. During mitosis, VRK remains chromatin-bound and active, and prevents reassociation of BAF by continuous phosphorylation. This model is similar to the proposed function of Cdk1 phosphorylation of LAP2 α . Mutant LAP2 α , which cannot be phosphorylated, associates constitutively with chromatin (Gajewski *et al*, 2004). Interestingly, phosphorylation of emerin in *Xenopus* mitotic extracts abolishes its binding to BAF (Hirano *et al*, 2005). Together, these data suggest that efficient dissociation of BAF, LEM proteins and chromatin during mitosis involves several phosphorylation events. In the absence of VRK, LEM proteins and the nuclear membranes in which they reside remain tightly associated with BAF and chromatin throughout mitosis. The result is that while nuclear membranes that are distinct from the ER can still form in the presence of mutant BAF-1 or in the absence of VRK-1, these membranes never get organized into a single, continuous NE. Contrary to previous suggestions on the role of BAF and LEM proteins (see Introduction), our data suggest that they are not needed for the segregation of membranes to the chromatin surface, but for the subsequent organization of these membranes into a continuous NE. Interestingly, an alternative means of binding nuclear membranes to chromatin, via direct interactions between DNA and INM proteins, was recently demonstrated (Ulbert *et al*, 2006). A corollary of the model described is that VRK phosphorylation of BAF must be turned off, or reversed by activations of phosphatase activities, when BAF, LEM proteins and NE membranes reassociate with chromatin during NE organization.

Localization of BAF and VRK changes during mitosis

We found that in late anaphase and telophase, BAF-1 and VRK-1, as previously shown for human BAF in HeLa cells (Haraguchi *et al*, 2001), initially localized to the entire chromatin surface, but then relocalized to a 'core' region at sites closely apposed to the spindle poles and midbody microtubules. With further progression through mitosis, the 'core' signal was further compressed and finally disappeared, leaving behind a weak overall NE rim signal. Whether this dynamic and rapid relocalization of BAF and VRK is important for coating the chromatin with membranes and for closing the NE is not yet known. One might however imagine that BAF may help to steer the ER membranes, as they coat the chromatin through its interactions with the transmembrane INM proteins, and this could be regulated by VRK.

Materials and methods

SNP mapping

SNP mapping (Wicks *et al*, 2001) was used to localize the *baf-1(t1639)* mutation (Gönczy *et al*, 1999). After crossing GE2576 with the Hawaiian strain CB4856, more than 500 recombinants were obtained and 11 SNPs on chromosome III were analyzed. Sequencing *baf-1(t1639)* worms revealed a single G→A substitution in the *baf-1* gene. An identical point mutation was identified in *baf-1(t1499)* animals (Gönczy *et al*, 1999).

RNA interference

RNAi was performed by feeding worms with bacteria that express double-stranded RNA (Askjaer *et al*, 2002). To analyze the effect of RNAi on viability, L4 larvae were incubated on RNAi plates at 20°C

for 24–72 h, as indicated, and transferred to individual plates for an additional 24 h. Adults were removed and hatching rate was measured after 1 day. The hatching rate of *baf-1(t1639)* embryos at 15–25°C was measured in the same way using OP50 control bacteria. To obtain *baf-1(RNAi)* and *vrk-1(RNAi)* embryos for imaging, unless otherwise specified in Results, L4 larvae from GFP strains were incubated on RNAi plates at 20°C for 72 and 24 h, respectively.

Development of a 'fast response mini-stage temperature controller'

To monitor *baf-1(t1639)* embryos continuously at permissive and restrictive temperature, or for rapid shifting between these temperatures, a Peltier element-based device was developed. This device allows variation of the sample temperature between 4 and 38°C at rates of ~1°C/s, and provides long-term temperature stability within $\pm 0.3^\circ\text{C}$ (<http://www.embl-em.de/products>; Gorjánác *et al*, 2007).

Live embryo imaging

Embryos were analyzed by using time-lapse fluorescent microscopy on a Perkin Elmer Spinning Disc Confocal Ultraspin RS microscope and by dual DIC and fluorescent microscopy on a Leica confocal microscope AOBS SP2 with HCX PL APO $\times 63/1.4$ objective. Images were collected at 7–20 s intervals.

For temperature shift experiments, worms were cultured at appropriate temperatures, as specified in Results. Worms were dissected in M9 buffer and mounted on 2% agarose between two coverslips, which were glued to the copper plate of the temperature controller unit with vacuum grease. Fluorescent and DIC images of embryos were collected at 20 s intervals on a Leica AOBS SP2 equipped with a microscope incubator box set at 20°C.

For dextran nuclear exclusion assays, 160 kDa dextran coupled to tetramethylrhodamine B isothiocyanate (Sigma-Aldrich) was injected into the gonads of worms, which were dissected 5 h later (Galy *et al*, 2003).

Immunofluorescence

Embryos were stained as described in Askjaer *et al* (2002), except that milk was substituted by 10% fetal calf serum as blocking agent in VRK-1 depletion and localization experiments. Antibodies are described in Supplementary data.

Transmission electron microscopy

C. elegans hermaphrodites-fed bacteria expressing either control, *baf-1* or *vrk-1* dsRNA were cryo-immobilized immediately using a Leica EM PACT high-pressure freezer (Leica, Vienna, Austria) and processed essentially as described in Franz *et al* (2005). Minor modifications are described in Supplementary data.

Supplementary data

Supplementary data are available at *The EMBO Journal* Online (<http://www.embojournal.org>).

Original movies corresponding to the still images presented in this manuscript are available at http://www.embl.org/research/groups/mattaj/baf-vrk_movies/index.html

Acknowledgements

We are grateful to S Winkler, G Ritter and J Rietdorf for collaboration on the fast response temperature controller, to T Zimmermann and S Terjung for assistance with microscopy, to S Leicht for help with 2D gel analysis, to S Wuerl for technical assistance, to Y Gruenbaum and KL Wilson for LEM-2 and emerin antibodies, to P Fontanet and M Torrent (CID-CSIC, Barcelona) for access to transformation equipment, to the EMBL Electron Microscopy Core Facility and G Griffiths for helpful discussions, to members of the Mattaj Laboratory for critical reading of the manuscript and to C González for generously providing research facilities for EK and PA. Some strains used in this work were provided by the *Caenorhabditis* Genetic Center funded by NIH. MG was funded by the Federation of European Biochemical Societies and Human Frontier Science Program Organization. EK was funded by a grant from the Spanish Ministry of Education and Science (BFU2004-01096) to PA, who also received funding from the Spanish Ramón y Cajal Programme (RYC-2003-001521) and EMBL.

References

- Aihara H, Nakagawa T, Yasui K, Ohta T, Hirose S, Dhomaie N, Takio M, Kaneko M, Takeshima Y, Muramatsu M, Ito T (2004) Nucleosomal histone kinase-1 phosphorylates H2A Thr 119 during mitosis in the early *Drosophila* embryo. *Genes Dev* **18**: 877–888
- Askjaer P, Galy V, Hannak E, Mattaj IW (2002) Ran GTPase cycle and importins alpha and beta are essential for spindle formation and nuclear envelope assembly in living *Caenorhabditis elegans* embryos. *Mol Biol Cell* **13**: 4355–4370
- Bengtsson L, Wilson KL (2006) Barrier-to-autointegration factor phosphorylation on Ser-4 regulates emerlin binding to lamin A *in vitro* and emerlin localization *in vivo*. *Mol Biol Cell* **17**: 1154–1163
- Cullen CF, Brittle AL, Ito T, Ohkura H (2005) The conserved kinase NHK-1 is essential for mitotic progression and unifying acentrosomal meiotic spindles in *Drosophila melanogaster*. *J Cell Biol* **171**: 593–602
- Franz C, Askjaer P, Antonin W, Iglesias CL, Haselmann U, Schelder M, de Marco A, Wilm M, Antony C, Mattaj IW (2005) Nup155 regulates nuclear envelope and nuclear pore complex formation in nematodes and vertebrates. *EMBO J* **24**: 3519–3531
- Furukawa K (1999) LAP2 binding protein 1 (L2BP1/BAF) is a candidate mediator of LAP2–chromatin interaction. *J Cell Sci* **112**: 2485–2492
- Furukawa K, Sugiyama S, Osouda S, Goto H, Inagaki M, Horigome T, Omata S, McConnell M, Fisher PA, Nishida Y (2003) Barrier-to-autointegration factor plays crucial roles in cell cycle progression and nuclear organization in *Drosophila*. *J Cell Sci* **116**: 3811–3823
- Gajewski A, Csaszar E, Foisner R (2004) A phosphorylation cluster in the chromatin-binding region regulates chromosome association of LAP2alpha. *J Biol Chem* **279**: 35813–35821
- Galy V, Mattaj IW, Askjaer P (2003) *Caenorhabditis elegans* nucleoporins Nup93 and Nup205 determine the limit of nuclear pore complex size exclusion *in vivo*. *Mol Biol Cell* **14**: 5104–5115
- Gant TM, Harris CA, Wilson KL (1999) Roles of LAP2 proteins in nuclear assembly and DNA replication: truncated LAP2beta proteins alter lamina assembly, envelope formation, nuclear size, and DNA replication efficiency in *Xenopus laevis* extracts. *J Cell Biol* **144**: 1083–1096
- Gerace L, Blobel G (1980) The nuclear envelope lamina is reversibly depolymerized during mitosis. *Cell* **19**: 277–287
- Giot L, Bader JS, Brouwer C, Chaudhuri A, Kuang B, Li Y, Hao YL, Ooi CE, Godwin B, Vitols E, Vijayadamar G, Pochart P, Machineni H, Welsh M, Kong Y, Zerhusen B, Malcolm R, Varrone Z, Collis A, Minto M, Burgess S, McDaniel L, Stimpson E, Spriggs F, Williams J, Neurath K, Ioime N, Agee M, Voss E, Furtak K, Renzulli R, Aanensen N, Carrrolla S, Bickelhaupt E, Lazovatsky Y, DaSilva A, Zhong J, Stanyon CA, Finley Jr RL, White KP, Braverman M, Jarvie T, Gold S, Leach M, Knight J, Shinkets RA, McKenna MP, Chant J, Rothberg JM (2003) A protein interaction map of *Drosophila melanogaster*. *Science* **302**: 1727–1736
- Gönczy P, Schnabel H, Kaletta T, Amores AD, Hyman T, Schnabel R (1999) Dissection of cell division processes in the one cell stage *Caenorhabditis elegans* embryo by mutational analysis. *J Cell Biol* **144**: 927–946
- Gorjánác M, Mattaj IW, Rietdorf J (2007) Some like it hot: switching biology on the microscope. *GIT Imag Micro* **9**: 26–27
- Gruenbaum Y, Lee KK, Liu J, Cohen M, Wilson KL (2002) The expression, lamin-dependent localization and RNAi depletion phenotype for emerlin in *C. elegans*. *J Cell Sci* **115**: 923–929
- Gruenbaum Y, Margalit A, Goldman RD, Shumaker DK, Wilson KL (2005) The nuclear lamina comes of age. *Nat Rev Mol Cell Biol* **6**: 21–31
- Haraguchi T, Koujin T, Segura-Totten M, Lee KK, Matsuoka Y, Yoneda Y, Wilson KL, Hiraoka Y (2001) BAF is required for emerlin assembly into the reforming nuclear envelope. *J Cell Sci* **114**: 4575–4585
- Heald R, McKeon F (1990) Mutations of phosphorylation sites in lamin A that prevent nuclear lamina disassembly in mitosis. *Cell* **61**: 579–589
- Hetzer MW, Walther TC, Mattaj IW (2005) Pushing the envelope: structure, function, and dynamics of the nuclear periphery. *Annu Rev Cell Dev Biol* **21**: 347–380
- Hirano Y, Segawa M, Ouchi FS, Yamakawa Y, Furukawa K, Takeyasu K, Horigome T (2005) Dissociation of emerlin from barrier-to-autointegration factor is regulated through mitotic phosphorylation of emerlin in a *Xenopus* egg cell-free system. *J Biol Chem* **280**: 39925–39933
- Ivanovska I, Khandan T, Ito T, Orr-Weaver TL (2005) A histone code in meiosis: the histone kinase, NHK-1, is required for proper chromosomal architecture in *Drosophila* oocytes. *Genes Dev* **19**: 2571–2582
- Lee KK, Haraguchi T, Lee RS, Koujin T, Hiraoka Y, Wilson KL (2001) Distinct functional domains in emerlin bind lamin A and DNA-bridging protein BAF. *J Cell Sci* **114**: 4567–4573
- Lew DJ, Burke DJ (2003) The spindle assembly and spindle position checkpoints. *Annu Rev Genet* **37**: 251–282
- Lin F, Blake DL, Callebaut I, Skerjanc IS, Holmer L, McBurney MW, Paulin-Levasseur M, Worman HJ (2000) MAN1, an inner nuclear membrane protein that shares the LEM domain with lamina-associated polypeptide 2 and emerlin. *J Biol Chem* **275**: 4840–4847
- Liu J, Lee KK, Segura-Totten M, Neufeld E, Wilson KL, Gruenbaum Y (2003) MAN1 and emerlin have overlapping function(s) essential for chromosome segregation and cell division in *Caenorhabditis elegans*. *Proc Natl Acad Sci USA* **100**: 4598–4603
- Liu J, Rolef Ben-Shahar T, Riemer D, Treinin M, Spann P, Weber K, Fire A, Gruenbaum Y (2000) Essential roles for *Caenorhabditis elegans* lamin gene in nuclear organization, cell cycle progression, and spatial organization of nuclear pore complexes. *Mol Biol Cell* **11**: 3937–3947
- Lopez-Borges S, Lazo PA (2000) The human vaccinia-related kinase 1 (VRK1) phosphorylates threonine-18 within the mdm-2 binding site of the p53 tumour suppressor protein. *Oncogene* **19**: 3656–3664
- Macaulay C, Meier E, Forbes DJ (1995) Differential mitotic phosphorylation of proteins of the nuclear pore complex. *J Biol Chem* **270**: 254–262
- Mansharamani M, Wilson KL (2005) Direct binding of nuclear membrane protein MAN1 to emerlin *in vitro* and two modes of binding to barrier-to-autointegration factor. *J Biol Chem* **280**: 13863–13870
- Margalit A, Segura-Totten M, Gruenbaum Y, Wilson KL (2005) Barrier-to-autointegration factor is required to segregate and enclose chromosomes within the nuclear envelope and assemble the nuclear lamina. *Proc Natl Acad Sci USA* **102**: 3290–3295
- Meier B, Ahmed S (2001) Checkpoints: chromosome pairing takes an unexpected twist. *Curr Biol* **11**: R865–R868
- Nichols RJ, Traktman P (2004) Characterization of three paralogous members of the mammalian vaccinia related kinase family. *J Biol Chem* **279**: 7934–7946
- Nichols RJ, Wiebe MS, Traktman P (2006) The Vaccinia-related kinases phosphorylate the N-terminus of BAF, regulating its interaction with DNA and its retention in the nucleus. *Mol Biol Cell* **17**: 2451–2464
- Peter M, Nakagawa J, Doree M, Labbe JC, Nigg EA (1990) *In vitro* disassembly of the nuclear lamina and M phase-specific phosphorylation of lamins by cdc2 kinase. *Cell* **61**: 591–602
- Piano F, Schetter AJ, Morton DG, Gunsalus KC, Reinke V, Kim SK, Kemphues KJ (2002) Gene clustering based on RNAi phenotypes of ovary-enriched genes in *C. elegans*. *Curr Biol* **12**: 1959–1964
- Prunuske AJ, Ullman KS (2006) The nuclear envelope: form and reformation. *Curr Opin Cell Biol* **18**: 108–116
- Rempel RE, Traktman P (1992) Vaccinia virus B1 kinase: phenotypic analysis of temperature-sensitive mutants and enzymatic characterization of recombinant proteins. *J Virol* **66**: 4413–4426
- Segura-Totten M, Kowalski AK, Craigie R, Wilson KL (2002) Barrier-to-autointegration factor: major roles in chromatin decondensation and nuclear assembly. *J Cell Biol* **158**: 475–485
- Segura-Totten M, Wilson KL (2004) BAF: roles in chromatin, nuclear structure and retrovirus integration. *Trends Cell Biol* **14**: 261–266
- Sevilla A, Santos CR, Barcia R, Vega FM, Lazo PA (2004a) c-Jun phosphorylation by the human vaccinia-related kinase I (VRK1) and its cooperation with the N-terminal kinase of c-Jun (JNK). *Oncogene* **23**: 8950–8958

- Sevilla A, Santos CR, Vega FM, Lazo PA (2004b) Human vaccinia-related kinase 1 (VRK1) activates the ATF2 transcriptional activity by novel phosphorylation on Thr-73 and Ser-62 and cooperates with JNK. *J Biol Chem* **279**: 27458–27465
- Shumaker DK, Lee KK, Tanhehco YC, Craigie R, Wilson KL (2001) LAP2 binds to BAF·DNA complexes: requirement for the LEM domain and modulation by variable regions. *EMBO J* **20**: 1754–1764
- Ulbert S, Platani M, Boue S, Mattaj IW (2006) Direct membrane protein–DNA interactions required early in nuclear envelope assembly. *J Cell Biol* **173**: 469–476
- Umland TC, Wei SQ, Craigie R, Davies DR (2000) Structural basis of DNA bridging by barrier-to-autointegration factor. *Biochemistry* **39**: 9130–9138
- Wicks SR, Yeh RT, Gish WR, Waterston RH, Plasterk RH (2001) Rapid gene mapping in *Caenorhabditis elegans* using a high density polymorphism map. *Nat Genet* **28**: 160–164
- Zheng R, Ghirlando R, Lee MS, Mizuuchi K, Krause M, Craigie R (2000) Barrier-to-autointegration factor (BAF) bridges DNA in a discrete, higher-order nucleoprotein complex. *Proc Natl Acad Sci USA* **97**: 8997–9002